

EXPERIENCES IN THE APPLICATION OF INTERMITTENCY DETECTION TECHNIQUES TO HOT-FILM SIGNALS IN TRANSITIONAL BOUNDARY LAYERS

Edward Canepa, Marina Ubaldi, Pietro Zunino
Dipartimento di Macchine, Sistemi Energetici e Trasporti - Università di Genova (Italy)

ABSTRACT

The present work originates from the need to select an intermittency detection method to be employed for the analysis of hot-film data in transitional boundary layers on turbine blade profiles. Several methods available in literature have been split in their basic common phases and the different algorithms and choices involved in each phase have been carefully analysed and compared. This operation has allowed to make appropriate changes to the algorithms and physically well based choices of the parameters, taking advantage also from the detailed experimental data produced by the authors.

INTRODUCTION

Surface hot-film instrumentation has proved to be an appropriate powerful tool for experimental studies of turbomachinery blade boundary layers. Different data processing procedures including statistical and frequency domain analysis techniques are currently applied to hot-film signals to gain information on boundary layer nature and development.

However most information coming out from these analyses has a semi-quantitative character which makes them relevant for the understanding of the physics of the phenomenon, but not directly incorporable in the transitional numerical simulation schemes. On the contrary quantitative information on the onset, development and end of transition is provided by the intermittency function which can be determined directly from the hot-film signals.

Several intermittency detection techniques have been proposed in literature, most of them was developed for hot-wire velocity signals, but they have been applied to hot-film $q\tau_w$ signals as well. Generally these procedures based on turbulent event detection algorithms require the definition of control parameters like threshold levels and smoothing times which make them dependent on the operator sensitivity and experience.

Purpose of the present contribution is to share the experience gained in the set up and application

of several intermittency detection methods to transitional boundary layers.

The hot-film data used for comparison and technique evaluation have been produced by the authors during detailed experimental investigations on gas and steam turbine profile transitional boundary layers (Ubaldi et al., 1996; Campora et al., 2000). Outline of the experiments and instrumentation is given in Table 1. Most investigations were completed by LDV boundary layer traverses that increase confidence in the use of hot-film information. The data are part of an ERCOFTAC and TRANSPRETURB Thematic Network database available at <http://transition.imse.unige.it/cases/>.

The initial idea was to choose among intermittency detection methods available in literature. After having studied and implemented different procedures it has been realised that the best strategy was not to compare results from the different methods and choose one of them; rather it seemed to be more appropriate to analyse and compare separately algorithms and choices adopted by the different methods. In fact most methods examined are composed of some common phases each involving appropriate algorithms or choices (Hedley and Keffer, 1974):

1. construction of a detector function $D(t, s)$ by processing the raw signal $q(t, s)$ to enhance the sensitivity to turbulent signatures;
2. use of a turbulent event detection algorithm in order to discriminate between turbulent and non-turbulent events, generating in most cases a criterion function $CR(t, s)$;
3. choice of a suitable window time T_w to be used within the detection algorithm, in order to avoid turbulent dropouts and remove laminar spikes;
4. choice of a suitable threshold S and comparison with the criterion function to construct an indicator function $\chi(t, s)$ which takes 1 when $CR(t, s) \geq S$ and takes 0 when $CR(t, s) < S$;
5. use of the square wave indicator function to perform conditional processing of each part of the signal;
6. long-term integration of the indicator function $\chi(t, s)$ (instantaneous intermittency) to obtain the cumulative intermittency function $I(s)$.

Table 1 Outline of the experiments and instrumentation

| Cascade Geometry | |
|------------------------------------|---|
| Chord length | $c = 300$ mm |
| Pitch to chord ratio | $g/c = 0.7$ |
| Aspect ratio | $h/c = 1.0$ |
| Inlet blade angle | $\beta'_1 = 0$ deg |
| Gauging angle | $\beta'_2 = \sin^{-1}(o/g) = 19.1$ deg |
| Number of blades | $N = 3$ |
| Test Conditions | |
| Inlet turbulence intensity | $Tu = 1\%$ |
| Inlet flow angle | $\beta_1 = 0$ deg |
| Outlet isentropic Reynolds numbers | $Re_{2c} = 1.6 \cdot 10^6$ and $5.9 \cdot 10^5$ |

Instrumentation

Single-sensor hot film gauge DANTEC 55R47
0.1x0.9 mm
CTA Dantec 55M10/55M17
Frequency response limit larger than 20 kHz from square-wave test
Low pass filter at 20 kHz
Signal acquisition at 40 kHz sampling rate, 12 bit resolution
Total number of data sampled for each measuring points 140000
pds performed by averaging 16 FFT performed using records of 8192 samples partially overlapping
Semiquantitative use of hot-film sensor:
evaluation of $q\tau_w = \left[\frac{(e^2 - e_0^2)}{e_0^2} \right]^3$ (Hodson, 1985) from the instantaneous CTA voltage $e(t)$

The intermittency detection methods differ in the many possible choices for detector function, window time and turbulent event detection algorithms, threshold level. In general some of these choices involve a certain degree of subjectivity.

The objective of the present work is to evaluate the different possibilities for each of the outlined phases and reduce the degree of subjectivity involved in the choice of S and T_w parameters.

SELECTION OF TURBULENT EVENT DETECTION ALGORITHM

In the present contribution four algorithms have been considered. The first one is the Direct Method (Hedley and Keffer 1974). The criterion function $CR(t, s)$ is generated by a smoothing process consisting in averaging the detector function $D(t, s)$ over a series of short time windows T_w . A turbulent event is detected if $CR(t,s) > S$. The short-term integration of the detector function causes loss of time resolution in the indicator

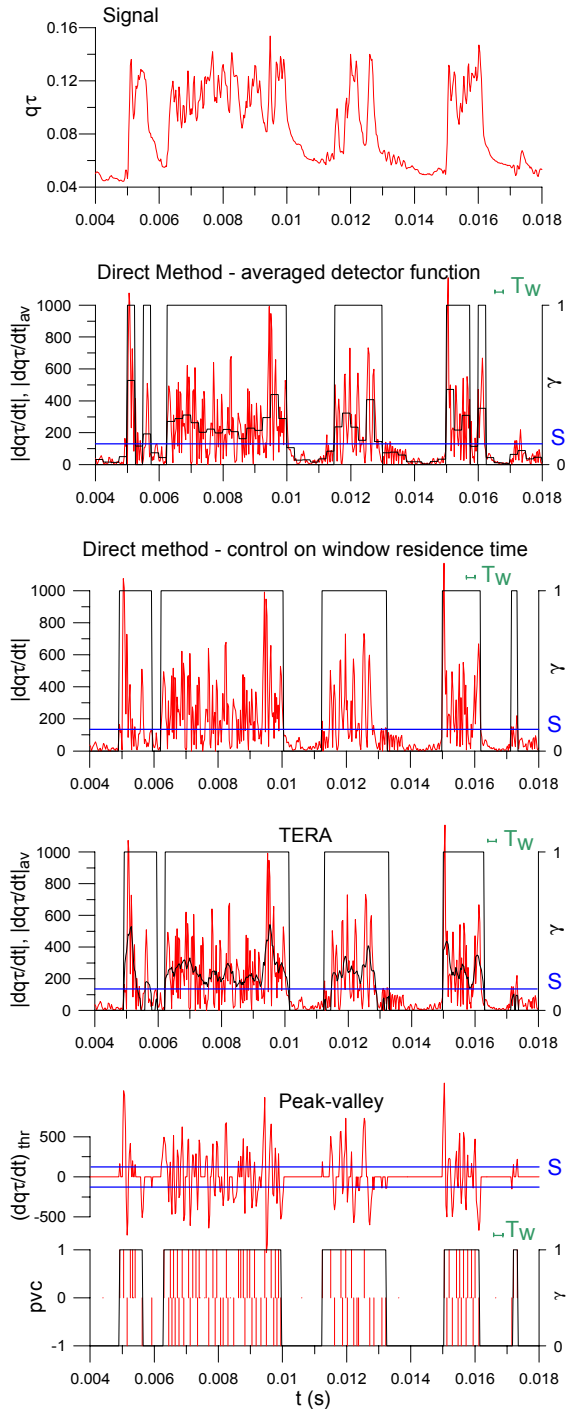


Fig. 1 Turbulent event detection algorithms.

function $\gamma(t)$ which is detrimental for conditional processing of the signal.

The second algorithm (Fasihfar and Johnson, 1992) is still a direct one but it is based on the control of the window residence time instead of averaging over a time window. A turbulent event is detected when $D(t, s)$ is greater than S . In order to fill in the dropouts, if $D(t, s) < S$ for a period shorter than T_w , then the signal is considered turbulent.

The third algorithm is the Turbulent Energy Recognition Algorithm (TERA), proposed by Falco and Gendrich (1990) and modified by Walker and

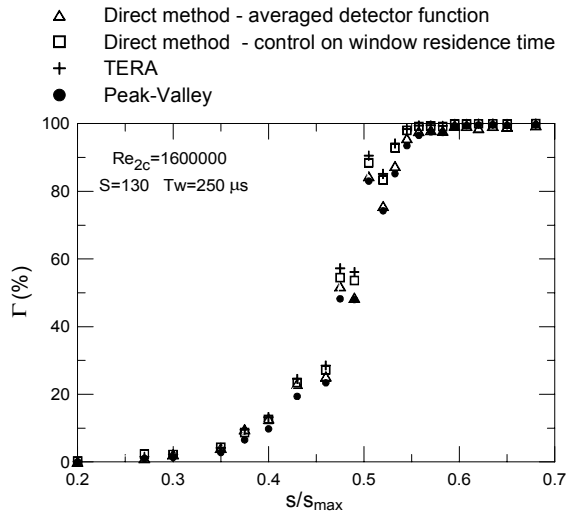


Fig. 2 Distributions of Γ for different turbulent event detection methods.

Solomon (1992). In this algorithm the turbulent event starts when $D(t, s) > S$, then the detection lasts until $D(t, s) > S$ or until $D(t, s)$ averaged over a short-time sliding window is larger than S . In order to fill the dropouts, if the period between two turbulent events is shorter than T_w the entire interval is considered as turbulent. If the turbulent event itself is shorter than T_w then it is considered as a laminar spike and removed.

The last algorithm considered is the Peak-Valley Counting (PVC) algorithm proposed by

Solomon (1996) where $D(t, s)$ is compared directly with S . If $D(t, s) < S$ then $D(t, s) = 0$. When a peak or a valley is found the peak and valley function assumes the values $pvc = \pm 1$. Thus a turbulent event is detected if the time between peaks and valleys is shorter than T_w . Besides if an entire turbulent event is shorter than T_w , it is removed as a laminar spike.

Figure 1 summarises the main characteristics of the different turbulent event detection methods. The raw signal $q\tau_w(t)$ is represented on the top of figure. The following four windows show for each method considered the typical approach, which starting from the same detector function $\partial(q\tau_w)/\partial t$ leads to the criterion function and the resulting indicator function $\gamma(t)$.

Figure 2 compares the distributions of cumulative intermittency function $\Gamma(s)$ obtained for the experiment at $Re_{2c} = 1.6 \cdot 10^6$ by the four algorithms, using the same time window $T_w = 250 \mu s$ and threshold level $S = 130$. Results are comparable but PVC method produces slightly lower values in transition region. That is due to a better evaluation of leading and especially trailing edges of turbulent spots. Figure 3 illustrates this concept: for the PVC Method turbulent spots appear shorter because the trailing edge relaxing zones of each spot are correctly recognised as non-turbulent.

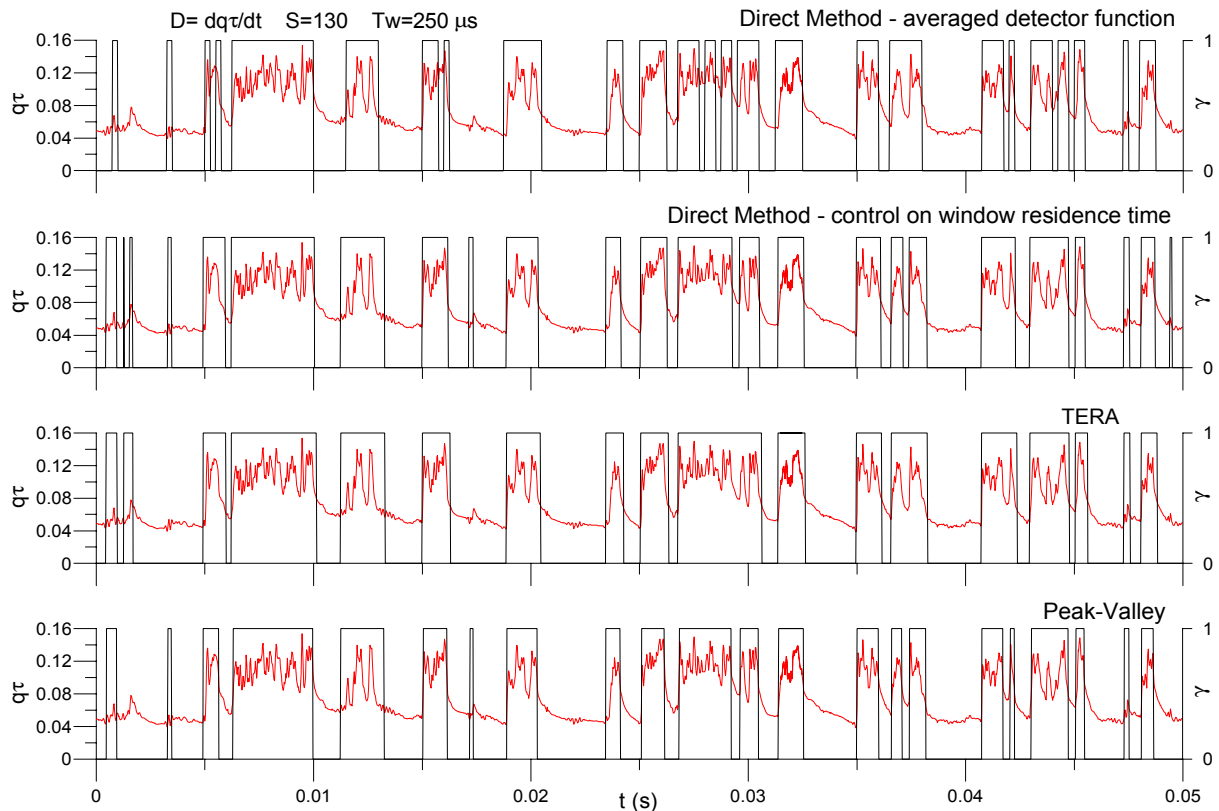


Fig. 3 Comparison of turbulent event detection methods: γ indicator function distributions.

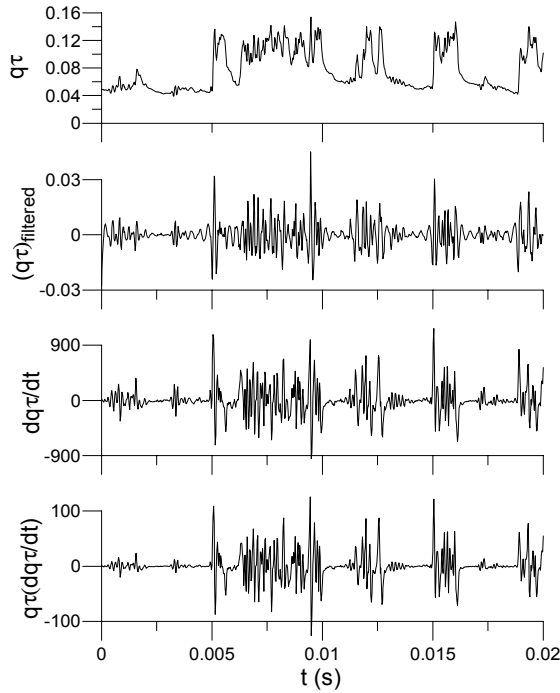


Fig. 4 Comparison of different detector functions.

COMPARISON OF DETECTOR FUNCTIONS

The detector function is obtained by processing the raw signal in order to accentuate the difference between turbulent and non-turbulent portion of the signal itself. Several function have been proposed in literature, depending also on the instrumentation employed (or physical quantity measured): single hot-wire (u), two-sensor hot-wire ($u \hat{v}$), hot-film ($q\tau_w$).

Our analysis is restricted to hot-film signal $q\tau_w$ and to the following three detector functions:

1. high pass filtered signal $(q\tau_w)_f$;
2. $\partial(q\tau_w)/\partial t$;
3. $q\tau_w \cdot \partial(q\tau_w)/\partial t$.

The function $(q\tau_w)_f$ corresponds to the commonly used high pass filtered output of the hot-wire anemometer u' . This function has been used by Gostelow and Blunden (1988), Fashifar and Johnson (1992).

The detector function $\partial(q\tau_w)/\partial t$ has been employed successfully by Solomon (1996) in connection with the PVC method and corresponds to the $\partial(u)/\partial t$ function used for hot-wire anemometer by several researchers, as reported by Hedley and Keffer (1974)

The function $q\tau_w \cdot \partial(q\tau_w)/\partial t$ is proposed in the present analysis. The multiplying factor $q\tau_w$ increases the discriminatory capability of the function $\partial(q\tau_w)/\partial t$, because $q\tau_w$ is large in the turbulent portion of the signal where also $\partial(q\tau_w)/\partial t$ is large. On the other hand it is low in

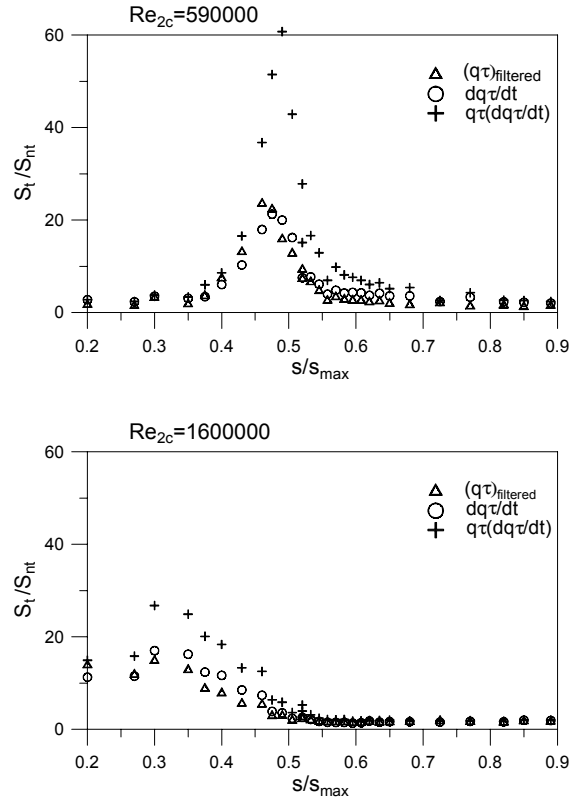


Fig. 5 Ratios of the conditionally averaged detector functions.

the non-turbulent portions where $\partial(q\tau_w)/\partial t$ is low too.

Figure 4 compares the different detector functions obtained from the raw signal $q\tau_w(t)$ shown on the top. Capability of the different functions to discriminate turbulent events can be evaluated by comparing by eye the relative amplitudes of turbulent and non-turbulent portions of the function. Function $q\tau_w \cdot \partial(q\tau_w)/\partial t$ looks superior because differences are more amplified than for the other functions. This criterion can be quantified by evaluating the ratio S_t/S_{nt} between the conditional time averages of the detector function over turbulent and non-turbulent portions (fig. 5).

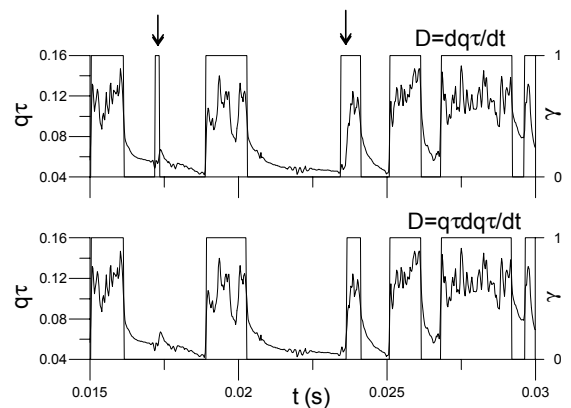


Fig. 6 Comparison of results obtained with different detector functions: γ indicator function distributions

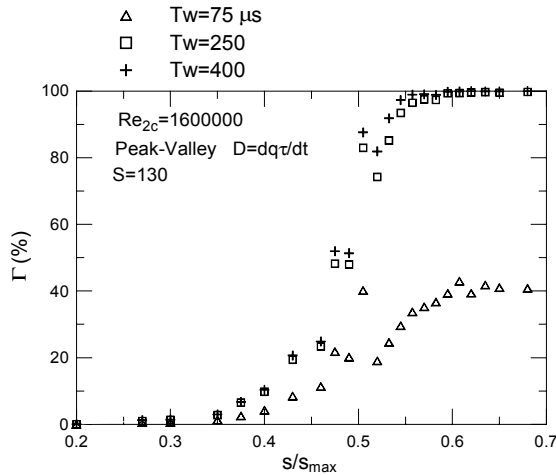


Fig. 7 Effect of time window T_w .

The larger values of S_i/S_{ni} for $q\tau_w \cdot \partial(q\tau_w)/\partial t$ result in a better resolution of the leading edge of the turbulent spots and correct recognition of laminar spikes (see arrows in fig. 6 showing γ indicator function distributions).

SELECTION OF THE WINDOW TIME T_w

The approaches available in literature to select the time window are many and differ significantly from each other, but it is possible to individuate three basic outlines.

The first one is by trial and error. Successive adjustments of time window can be made by inspection of the time trace of signal windowed by the indicator function $\gamma(t)$ or monitoring the streamwise distribution of cumulative intermittency function $\Gamma(s)$. In literature values of the time window vary from 80 μs to 500 μs in a large range of Reynolds numbers of the experiments. Some authors quote the window time in terms of sampling intervals, from 3 to 10 Δt_s . Figure 7 shows the significant effect of the T_w choice on the intermittency distribution $\Gamma(s)$. The most suitable value for this experiment is $T_w = 250 \mu s$.

The second approach stems from the definition of T_w in terms of convective time scale of the

boundary layer $T_{bl} = \delta/u_e$, some examples are:

Fasihfar and Johnson (1992) $T_w = 2\pi T_{bl}$;

Hazarika and Hirsch (1995) $T_w = T_{bl} \div 2T_{bl}$;

Walker and Solomon (1992) $T_w = (0.4 \div 3.5) T_{bl}$.

Suitable values found for the present test cases are $T_w = 8 T_{bl}$ for $Re_{2c} = 1600000$ and $T_w = 3.7 T_{bl}$ for $Re_{2c} = 590000$.

An other approach considers T_w as a multiple of the Kolmogorov time scale T_k . Some examples are:

Hedley and Keffer (1974) $T_w/T_k = 28$ (edge intermittency).

Kuo and Corsin (1971) $T_w/T_k = 15 \div 35$ (edge intermittency).

Blair (1992) $T_w/T_k = 150$ (transitional boundary layer).

Keller and Wang (1995) $T_w/T_k = 200$ (transitional boundary layer).

Suitable values for the present test cases give $T_w = 550 T_k$ for $Re_{2c} = 1600000$ and $T_w = 250 T_k$ for $Re_{2c} = 590000$. Here T_k has been evaluated from the relationship $T_l/T_k = Re_t^{3/4}$ (Turns, 1996), where T_l is the integral time scale and Re_t is a turbulence

Reynolds number $Re_t = (\overline{u'^2})^{1/2} \cdot (U_e \cdot T_l) / \nu$.

The large range of variation of T_w in literature, partly depends on the different turbulent detection scheme adopted, but especially it is due to the different type of intermittency investigated and to the large variation of Reynolds number (for example the ratio T_l/T_k varies from 178 to 1000 when Re_t varies from 1000 to 10000).

On the basis of the present experience, two criteria are proposed in order to discriminate between the smallest frequencies (large eddies) of the turbulent fluctuations and the highest frequencies of the non-turbulent flow fluctuations (laminar instabilities, low frequency flow unsteadiness, laminar-turbulent intermittency).

The time window T_w can be assumed as the time integral scale T_l of the turbulent portion of the signal, physically it is the mean period of the large fluctuations in the turbulent flow. In practice T_l is evaluated from the power density spectrum of $q\tau_w$

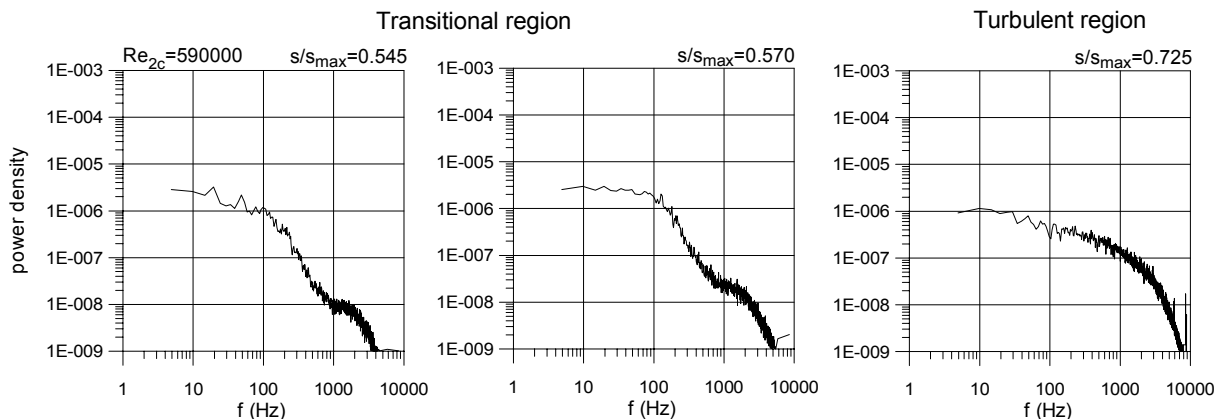


Fig. 8 Power density spectra of $q\tau_w$ in transitional and turbulent regions

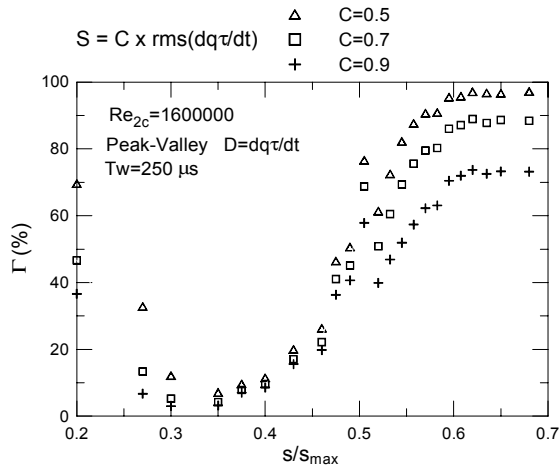


Fig. 9 Effect of threshold level definition based on the long-term rms of the detector function.

at the first station after turbulent completion:

$$T_I = \frac{S_{uu}(0)}{4 \cdot u'^2} \quad (\text{Cebeci and Smith, 1974}).$$

$T_I = 400 \mu\text{s}$ for $\text{Re}_{2c} = 590000$; and $T_I = 200 \mu\text{s}$ for $\text{Re}_{2c} = 1600000$. For $\text{Re}_{2c} = 590000$, T_I evaluated from $q\tau_w$ power density spectrum is approximately equivalent to the value obtained from the power density spectrum of u measured with LDA at $y^+ = 10$.

An alternative way for discriminating between the smallest frequencies of the turbulent portion and the largest frequencies of the non-turbulent portion is based on the direct inspection of the power density spectra in the transition region (fig. 8). Energy spectra (plotted in logarithmic scale) show a change of slope at a particular frequency f_c which identifies the increase of energy in the low frequency range due to the laminar-turbulent intermittency.

For the PVC scheme we assume T_w equal to half of the period of the lowest frequency turbulent fluctuation $T_w = 1/(2f_c)$.

For the present experiments at $\text{Re}_{2c} = 590000$ the value of the cutting frequency was $f_c = 1000 \text{ Hz}$ and the window time was $T_w = 500 \mu\text{s}$, at $\text{Re}_{2c} = 1600000$ the values were $f_c = 2500 \text{ Hz}$ and $T_w = 200 \mu\text{s}$.

SELECTION OF THRESHOLD LEVEL

In order to select a threshold level the first possible approach is by trial and error, making successive adjustments of level by inspection of the time trace of signal, windowed by the indicator function γ . Alternatively, looking at the streamwise distribution of cumulative intermittency, a suitable threshold level is obtained by trial and error imposing the achievement of boundary conditions $\Gamma = 1$ after turbulent completion and $\Gamma = 0$ before transition's beginning. This procedure has been

adopted in several works, but it is time consuming because not automatic, and somehow arbitrary.

The second possible method is to define S as a percentage of the long-term rms of the detector function or the long-term average of the signal itself. This threshold level $S = C \text{ rms}(D(t))$ is typical of the TERA method of Falco and Gendrich (1990), but has been widely used also in other methods (e.g. Blair, 1992; Walker and Solomon, 1992). This method causes non-zero values of the Γ function in the laminar zone and too large values at the beginning of transition (fig. 9). An increase of the constant C to reduce the Γ values results in unrealistic non unity values in the turbulent region.

The third approach is defined Dual Slope Method (Keller and Wang, 1995) and requires the intermittency to be drawn as a function of the threshold level for each measuring point. The level is selected at the intersection of two straight lines approximating the intermittency distribution. Identification of the two straight lines is not always possible especially near completion of transition. The method is exemplified in fig. 10. Values of the cumulative intermittency function $\Gamma(s)$ obtained by the Dual Slope method appear much larger than those obtained using the most suitable value of the threshold level for the present experiment ($S=130$). The method fails especially in the low intermittency region near the beginning of

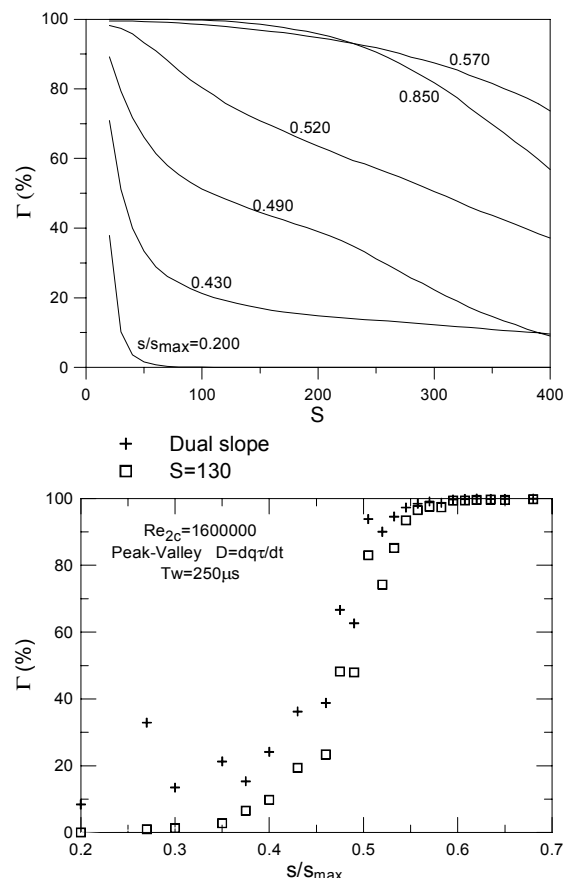


Fig. 10 Application of the Dual Slope method for threshold level selection.

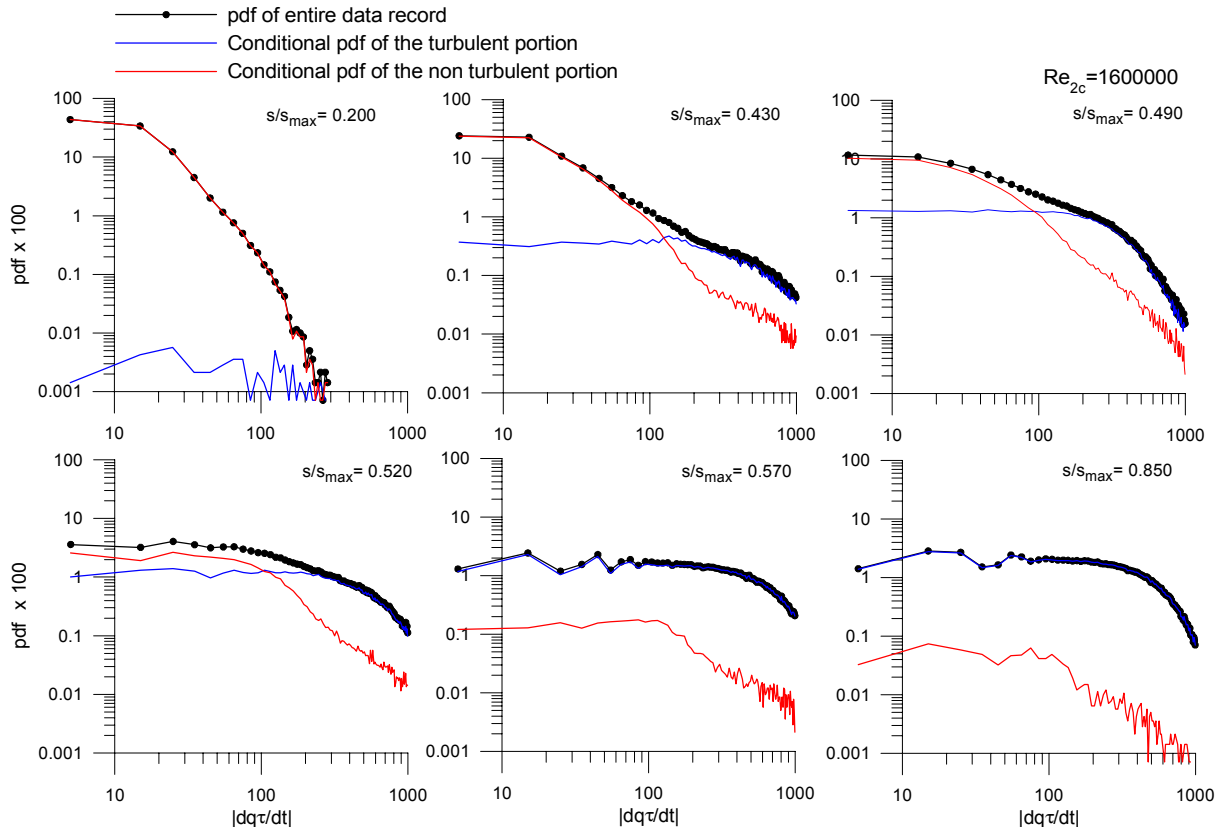


Fig. 11 Conditional and global probability density functions of $\partial(q\tau_w)/\partial t$ for threshold level selection.

transition.

In the last approach the S level selection is made on the basis of the probability density function (pdf) of the detector function or other correlated functions (Hazarika and Hirsch, 1995; Kalfas and Elder, 1995; Solomon, 1996). The level is selected at the intersection of the two conditional probability density functions, one for the turbulent portion and the second for the non-turbulent one, where the minimum probability of incorrect identifications is supposed. This procedure is exemplified in fig. 11. This approach is non arbitrary and physically well based and has been here evaluated to be the best criterion, but there's the necessity of an initial assumption for the threshold level to separate the turbulent portion from the non-turbulent one, in order to allow the conditional pdf evaluation. Furthermore the approach is not applicable at the beginning and at the end of the transition because of the absence of intersection between turbulent and non-turbulent conditional pdf, as shown in fig. 11 ($s/s_{max} = 0.20$; 0.57 ; 0.85). Some practical suggestions that come out from our analysis can be applied to overcome the above mentioned difficulties.

An initial assumption for the threshold level can be chosen by analysing the probability density function of the entire signal in the transition region looking for a change of curvature of the distribution on the turbulent side (point where the

pdf distribution of turbulent events starts to separate from the pdf of the entire data record, fig. 11 $s/s_{max}=0.430$ and $s/s_{max}=0.490$), instead of using the most common approach with the level S defined as a percentage of the long-term rms of the detector function.

The threshold levels for the beginning and completion of transition can be extrapolated from the values coming out from the pdf distribution of the measuring points in the central region of the transition length. In the present experiments constant values of S were assumed.

For the proposed detector function $q\tau_w \cdot \partial(q\tau_w)/\partial t$ the threshold level is evaluated as the threshold level of $\partial(q\tau_w)/\partial t$ multiplied by the long-term average of $q\tau_w$.

INTERMITTENCY EVALUATION PROCEDURE BASED ON PDF OF $q\tau_w$

The hot-film signal $q\tau_w$ presents a higher sensitivity compared with the single hot-wire signal u and one can try to discriminate turbulent and non-turbulent states by analyzing the pdf of the $q\tau_w$ signal without the necessity of producing a detector function and using a recognition algorithm (PDF method of Schneider, 1995).

The method has been implemented in the present work by means of a least squares fitting of the turbulent portion of the pdf.

$Re_{2c}=1600000$

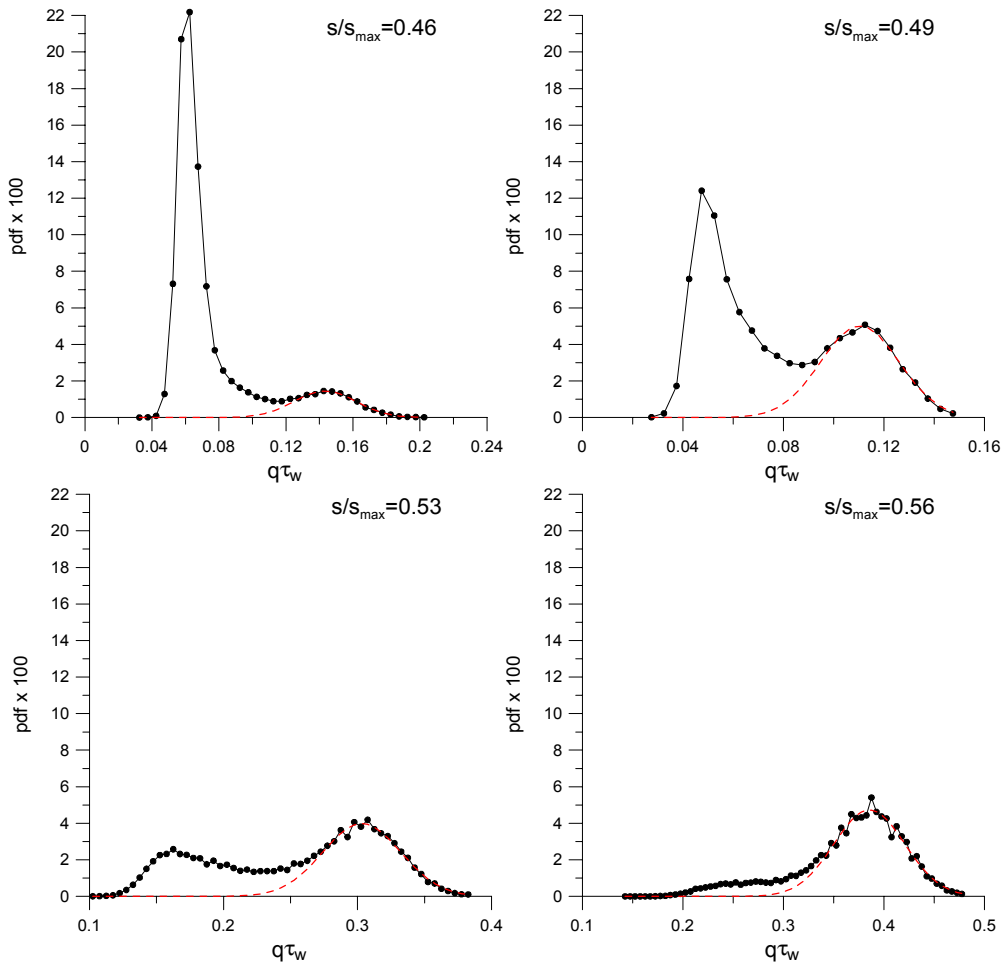


Fig. 12 Application of PDF method.

$$P(x) = A_1 \exp \left[- \left(\frac{x - A_2}{A_3} \right)^2 \right]$$

where A_1 amplitude, A_2 centre and A_3 width of the Gaussian fit are obtained using a non-linear least squares routine based on Levenberg-Marquardt method (Press et al., 1992). The minimum value of $q\tau_w$ for the turbulent portion of the data record pdf, located in the valley between high and low shear portions, is defined iteratively in order to obtain the best fit.

The cumulative intermittency is calculated as

$$\Gamma = \int P(x) dx = A_1 A_3 \sqrt{\pi}$$

Figure 12 shows the application of the PDF method to the $Re_{2c}=1600000$ experiment.

Figure 13 compares the Γ distribution obtained by the PDF method with that obtained by the PVC method: pdf distribution is slightly lower. This feature is explained in fig. 14: the conditional pdf of the turbulent events produced by the PVC method presents a significant tail towards the lowest $q\tau_w$ values where the PDF method postulates a Gaussian distribution. The discrepancy can be

due to the fact that in PVC method the detector function, being based on first derivative of the signal, includes the spot edges in the turbulent portion of the signal.

The simple PDF method is efficient and does not require subjective choices, but not in all the experiments the ratio between turbulent and non-turbulent values of $q\tau_w$ is high enough to find the

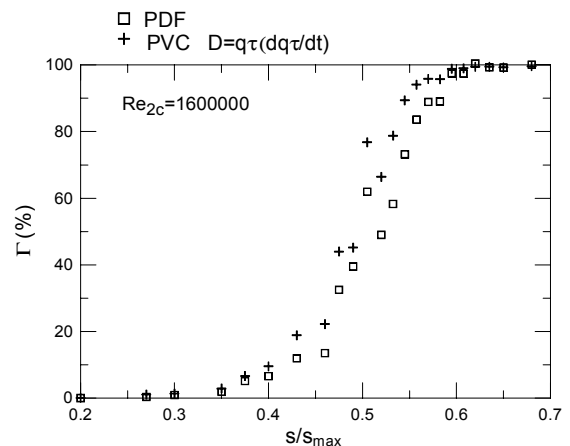


Fig. 13 Comparison of PDF and PVC methods.

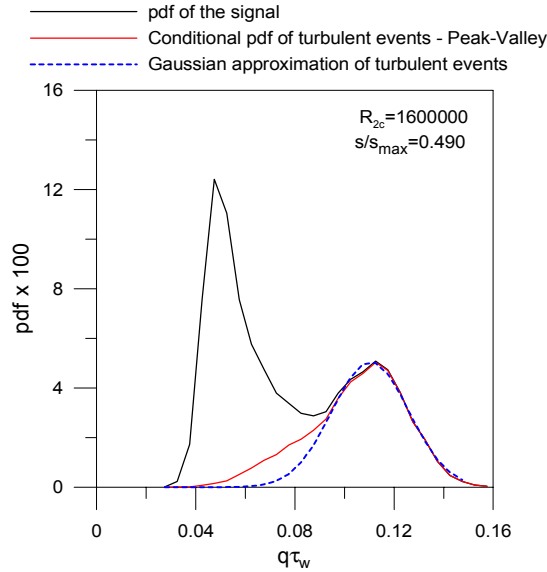


Fig. 14 Comparison of pdf distributions.

intermittency evaluation on the pdf distribution, without using a detector function to enhance sensitivity. Besides the major drawback of this method is the non availability of an instantaneous indicator function $\chi(t)$ to be used for conditional processing of the signal (conditional pds or wavelet processing of data, ensemble averages in presence of periodic perturbations).

CONCLUSIONS

Several intermittency evaluation methods have been considered and analysed in order to find out the less subjective approaches suitable for processing results of an hot-film transitional boundary layer investigation.

The simple PDF method based on the direct statistical analysis of the $q\tau_w$ signal was found to be suitable for separating turbulent and non-turbulent events for the present experiments. However, this result cannot be generalised since pdf distributions of $q\tau_w$ at low Reynolds numbers may present less accentuate difference between turbulent and non-turbulent parts.

The detailed analysis of the different choices involved in the common basic stages which constitute most methods based on the analysis in time of a detector function has given the following results.

- All the detector functions examined show suitable discriminatory capability. The function $q\tau_w \cdot \frac{\partial(q\tau_w)}{\partial t}$ proposed in the present work gives a higher S_t/S_{nt} ratio respect to the other functions. The detection of the leading edge of turbulent spots and the recognition of laminar spikes are more precise.
- All the examined turbulent event detector algorithms show acceptable results. The PVC

algorithm presents the best capability in discriminating the relaxing portions of signal at the trailing edge of turbulent spots.

- Among the threshold level evaluation techniques, the pdf based selection procedure is the less subjective and more physically based, but requires an initial evaluation of the threshold. The present analysis suggests that a suitable choice of the initial value can be done on the basis of the non-conditional pdf.
- Window time depends strongly on the time-varying structure of the turbulent flow which varies significantly with the Reynolds number of the experiment. Indications from literature give rise to a large range of values. A non subjective measure of the mean time of the largest turbulent eddies is the integral time scale of the turbulent portion of the flow. The estimation of this time scale based on the pds of the $q\tau_w$ signal after the transition completion fits well with the turbulent event detection procedure for both Reynolds numbers considered. In the present experiments the integral time scale of turbulent flow is nearly coincident with one half of the period corresponding to the increase of energy at lower frequencies in the pds of the $q\tau_w$ signal taken in the transitional region. This appears as a practical, physical based, criterion to be used with the PVC procedure.

NOMENCLATURE

| | |
|--------------|---|
| c | blade cord length |
| D | detector function |
| e | hot-film signal |
| e_0 | hot-film signal at zero flow condition |
| pvc | peak and valley function |
| $q\tau_w$ | quasi wall shear stress |
| Re_t | turbulence Reynolds number |
| Re_{2c} | Reynolds number based on cascade outlet velocity and chord length = $u_2 c / \nu$ |
| S | threshold level |
| S_{uu} | power spectral density |
| S_t/S_{nt} | ratio between turbulent and non-turbulent time averages |
| s | surface distance measured from the leading edge |
| s_{max} | surface length from leading to trailing edge |
| T_k | Kolmogorov time scale |
| T_I | integral time scale |
| T_w | window time |
| t | time |
| u_e | local free-stream velocity |
| u_τ | wall friction velocity |
| u' | velocity fluctuation in streamwise direction |
| y | normal distance from the wall |
| y^+ | dimensionless distance from the wall = yu_τ/ν |
| Γ | cumulative intermittency function |

| | |
|--------------|--------------------------------------|
| γ | instantaneous intermittency function |
| Δt_s | sampling interval |
| δ | boundary layer thickness |
| ν | kinematic viscosity |

ACKNOWLEDGMENTS

This work has been supported by CEC through TRANSPRETURB Thematic Network.

REFERENCES

Blair, M. F., 1992, "Boundary layer transition in accelerating flows with intense free stream turbulence: Part 2-The zone of intermittent turbulence", ASME Journal of Fluids Engineering, vol. 114, pp. 322-332.

Campora, U., Pittaluga, F., Ubaldi, M., Zunino, P., 2000, "A detailed investigation of the transitional boundary layer on the suction side of a turbine blade.", Proc. XV Bi-Annual Symposium on Measuring Techniques in Transonic and Supersonic Flows in Cascades and Turbomachines, Firenze, Italy.

Cebeci, T., Smith, A. M. O., 1974, "Analysis of turbulent boundary layers", Academic Press.

Fasihfar, A., Johnson, M. W., 1992, "An improved boundary layer transition correlation", ASME Paper No. 92-GT-245.

Falco, R.E., Gendrich, C.P., 1990, "The turbulence burst detection algorithm of Z. Zaric", 1988 Zoltan Zaric Memorial Conference on Near-Wall Turbulence, Hemisphere, pp.911-931.

Gostelow, J. G., Blunden, A. R., 1988, "Investigation of boundary layer transition in an adverse pressure gradient", ASME Paper No. 88-GT-2.

Hazarika, B. K., Hirsh, C., 1995, "Transition over C4 leading edge and measurement of intermittency factor using PDF of hot wire signal.", ASME Paper No. 95-GT-294.

Hedley, T. B., Keffer, J. F., 1974, "Turbulent/non-turbulent decisions in an intermittent flow.", J. Fluid. Mech., Vol. 64, part 4, pp. 625-644.

Hodson, H. P., 1985, "Boundary-Layer Transition and Separation near the Leading Edge of a High Speed Turbine Blade", ASME Journal of Engineering for Gas Turbine and Power, vol. 107, pp. 127-134.

Kalfas, A. I., Elder, E. L., 1995, "Determination of the intermittency distribution in the boundary layer of a flat plate with C4 leading edge", ERCOFTAC Bulletin No. 24.

Keller, F. J., Wang, T., 1995, "Effects of Criterion Function on Intermittency in Heated Transitional Boundary Layers With and Without Streamwise Acceleration", ASME Journal of Turbomachinery, vol. 117, pp. 154-165.

Kuo, A.Y., Corsin, S., 1971, "Experiments on internal intermittency and fine structure distribution

The 16th Symposium on Measuring Techniques in Transonic and Supersonic Flow in Cascades and Turbomachines

functions in fully turbulent fluid", J. Fluid. Mech., Vol. 50, pp. 285-319.

Press, W. H., Teukolsky, S. A., Vetterling, W.T., Flannery, B. P., 1992, "Numerical Recipes", Cambridge University Press.

Schneider, S. P., 1995, "Improved methods for measuring laminar-turbulent intermittency in boundary layers.", Experiments in Fluids vol. 18, pp. 370-375.

Solomon, W. J., 1996, "Unsteady boundary layer transition on axial compressor blades.", Ph. D. thesis, University of Tasmania, Hobart.

Turns, S.R., 1996, "An Introduction to Combustion - Concepts and Applications", Mc Graw Hill Inc.

Ubaldi, M., Zunino, P., Campora, U., Ghiglione, A., 1996, "Detailed velocity and turbulence measurements of the profile boundary layer in a large scale turbine cascade.", ASME Paper No. 96-GT-42.

Walker, G. J., Solomon, W. J., 1992, "Turbulent intermittency measurements on an axial compressors blade", 11th Australian Fluid Mechanics Conference, vol. II, pp. 1277-1280.